

ST. NO. 23837  
CoA. Note No. 423  
LTH



THE COLLEGE OF AERONAUTICS  
CRANFIELD



A PRELIMINARY EXPERIMENTAL INVESTIGATION OF THE  
EFFECT OF SURFACE CATALYTIC EFFICIENCY ON  
STAGNATION POINT HEAT TRANSFER

by  
J. R. Busing

23837



3 8006 10057 7280

NOTE NO. 123

January, 1962.

THE COLLEGE OF AERONAUTICS  
CRANFIELD

\* A Preliminary Experimental Investigation of the  
Effect of Surface Catalytic Efficiency on  
Stagnation Point Heat Transfer

- by -

J. R. Busing, B.E., B.Sc., D.C.Ae.

SUMMARY

Results of an experimental investigation to measure the difference between the heat transfer rate to a catalytic wall and to a non-catalytic wall are presented. Using thin film thermometer techniques, associated with an electrical analogue, direct measurement was made of the heat transfer rate to a chemically deposited platinum film and a vacuum evaporated silicon monoxide film. These films were formed near the stagnation point of a pyrex glass sphere and the experiments were done in the College of Aeronautics shock tube. The models were designed so that the heat transfer rates were measured under identical flow conditions.

The results obtained indicate that the heat transfer rate to the platinum film is significantly higher than the heat transfer rate to the silicon monoxide film.

---

\* This report was presented at the Fifth Scientific Conference of the Polish Academy of Sciences, Jablonna, Poland. 1961.



## CONTENTS

	<u>Page</u>
Summary	
1. Introduction	1
2.1. Shock Tubes	1
2.2. Models	2
2.3. Instrumentation	3
3. Theory	3
4. Results	5
5. Comparison of Theoretical and Experimental Results	6
5.1. The flow in the boundary layer is not frozen	6
5.2. Incorrect value for the catalytic activity of silicon monoxide	6
5.3. The flow outside the boundary layer is not in equilibrium	7
6. Acknowledgements	7
7. References	8
Figures	

## 1. Introduction

Stagnation temperatures encountered by hypersonic vehicles and re-entry satellites are of the order of several thousands of degrees Kelvin. This introduces a severe heating problem, particularly at the stagnation point.

At these elevated temperatures the gas behind the bow shock wave is highly dissociated. Thus, in addition to the normal aerodynamic heating by molecular conduction one must consider the effect upon the heat transfer of the diffusion of atoms and the energy that they liberate upon recombination. If the density is sufficiently low, the atoms may diffuse across the boundary layer and reach the wall before recombining, i. e. the flow is "frozen". They may then recombine on the wall and the energy thus liberated could greatly increase the rate of heat transfer to the surface. Conversely, if a wall of low catalytic activity is used then the heat transfer rate should be considerably reduced.

Stagnation conditions which are developed in flight can be reproduced in the shock tube and considerable work has been done on high temperature gas flows with this specialised facility.

The effect of dissociation in such flows has been extensively studied both theoretically and experimentally. A theory of stagnation point heat transfer has been developed notably by Lees (Ref. 1) and by Fay and Riddell (Ref. 2). Experimental investigations have been performed by Rose and Stark (Ref. 3) and many others, which confirm the theoretical predictions.

It has been pointed out in theoretical studies by Scala (Ref. 4) and Goulard (Ref. 5) that the catalytic efficiency of the surface can have a strong influence on the heat transfer. That is, the higher the catalytic efficiency of the surface, the more easily do atoms recombine there and liberate their energy of dissociation.

The experiments to be described later have been designed to produce flows with a high degree of dissociation at relatively low densities, in an attempt to produce frozen conditions in the boundary layer. Thin film thermometers have been used to measure heat transfer rates to a bare platinum film and also to a platinum film coated with silicon monoxide. These two films should have different catalytic efficiencies and hence there should be different heat transfer rates to them under frozen flow conditions.

### 2. 1. Shock Tubes

The unsteady flow which is set up in a shock tube, when the diaphragm separating high pressure from low pressure bursts, is well understood and is illustrated in Fig. 1.

This idealised flow diagram is modified in practice by the effect of viscosity and the associated boundary layer which forms behind the moving shock wave. The contact surface is accelerated and diffuses rapidly into the hot region. As a result the length of hot flow is considerably reduced. These effects are most severe at low densities.

The College of Aeronautics shock tube is made from stainless steel of 5 cm. internal diameter and about one cm. wall thickness. The tube is mounted vertically with the high pressure section at ground level and the working section at first floor

level. The dump chamber and vacuum equipment are on the second floor. The main dimensions are shown in Fig. 2. Fig. 3a shows the charging equipment which is remotely controlled from the first floor and the high pressure section which can be swung to one side to change diaphragms, whilst Fig. 3b shows the dump tank, diffusion pump, backing pump and control valves. Fig. 4a shows a close up of the model mounted in the working section in the unexpanded flow, and Fig. 4b is a view of the working section and associated electronic equipment for recording initial tube pressure, shock velocity and heat transfer rates.

Diaphragms of various thicknesses made from pure copper, aluminium or plastic film are used. The metal ones are prescribed to ensure symmetrical petalling without loss. The diaphragms are allowed to burst naturally using cold hydrogen as the driver gas at pressures up to 75 atmospheres. The channel or low pressure section of the tube is normally evacuated to about  $10^{-4}$  Torr and air or other gas admitted to the desired pressure. The pressures rise in the system due to leaks is about  $10^{-3}$  Torr per minute. This is acceptable at initial pressures of 0.05 Torr. Pressures are measured with an "Alphatron" vacuum gauge which depends for its operation on the variation of alpha ray absorption with change of gas pressure. This gauge will measure total pressures in the range 1000 Torr to  $10^{-3}$  Torr with accuracies of about 2%.

Shock velocity is measured by recording on a microsecond counter the time interval required for the shock to travel 20 cm. The shock wave is detected by thin film resistance thermometers, which give reliable triggering at Mach numbers as low as 1.1 into air at 200 Torr. (This corresponds to detection of a temperature rise of about  $0.05^{\circ}\text{C}$  at the wall).

## 2.2. Models

All the models used were made from 1.27 cm. diameter polished pyrex glass spheres. The heat transfer gauges were thin film resistance thermometers formed from platinum paint (Hanovia 05X) baked onto the pyrex at a temperature near the softening point of the glass. The films were approximately  $10^{-4}$  mm. thick and about 0.2 mm. wide. They were drawn as an open circle approximately 1.2 mm. dia. around the geometric stagnation point. This corresponds to a  $10^{\circ}$  angle subtended at the sphere centre. The temperature coefficient of resistance of the films was 2.5 milliohms/ohm per  $^{\circ}\text{C}$ . Gauge resistances were about 100 ohms and were used with a steady current of 15 milliamps flowing through them. Copper plated platinum leads were used to connect the signal wires to the gauge.

Initially, a single gauge was used with either bare platinum or silicon monoxide coated platinum as the sensing element. However, it was found that identical flow conditions could not be reproduced in the shock tube at low densities and so a model having two sensing elements was made. Figure 5 shows the two types of model and the method of mounting in the working section. The silicon monoxide was deposited by vacuum evaporation and in thicknesses of about  $5 \times 10^{-5}$  mm. was very adherent and remarkably robust.

These models lasted for five or six runs, after which the gauge was open circuited probably by a direct hit from a dust particle carried along by the contact surface.

### 2.3. Instrumentation

When measuring heat transfer rates in a shock tube it is usual to record the surface temperature variation with time by means of a thin film resistance thermometer. A fairly lengthy numerical integration of points read off the film is then required to obtain the variation of heat transfer rate with time. Meyer (Ref. 6) has suggested the use of the electrical analogue for the direct measurement of heat transfer rate. He has used his design successfully in a gun tunnel. A similar analogue, but with much shorter time resolution, has been used in these experiments and is shown in Fig. 6. The diffusion of charge into this network closely approximates to the diffusion of heat into a semi-infinite solid. Hence, the voltage developed across the first resistor is directly proportional to the heat transfer rate. The sensitivity of this network is such that a heat transfer rate of 100 watts/cm<sup>2</sup> will give an output of one millivolt. In practice this network will show variations in heat transfer rates which are impossible to obtain from the temperature records because of the inaccuracies in film reading and integration. Fig. 7 shows the temperature record and equivalent heat transfer rate obtained via the analogue network.

The circuit for recording the heat transfer rates from the composite model is shown diagrammatically in Fig. 8. The power supply and balance network were used to equalise the output from the two gauges and also to adjust the gauge voltage in the event of the resistance increasing during a run.

Since heat transfer rates could be measured directly the models were calibrated in the shock tube at a low shock Mach number. The heat transfer rates were calculated using Fay and Riddell's result and the gauge sensitivities determined.

### 3. Theory

The boundary layer equations, including the effect of chemical dissociation, have been formulated by Lees, (Ref. 1) and Fay and Riddell (Ref. 2). They considered that heat is transferred to the wall by normal molecular conduction and in addition by diffusion of atoms which recombine, either in the gas stream or on the wall. There are two extremes possible - a very fast recombination rate in which the gas is in equilibrium throughout the boundary layer or a slow recombination rate where the atom concentration remains constant through the layer. For these two extreme cases Lees simplified the boundary layer equations and then solved them approximately. Fay and Riddell solved the equations numerically for all values of the recombination rate. Both Lees and Fay and Riddell, however, assumed that the boundary condition at the wall was that the atom concentration is zero; this corresponds to an infinitely efficient catalyst.

In general Goulard (Ref. 5) assumed that the atom concentration at the wall must be greater than zero. From mass conservation principles he deduced that, for equilibrium, the mass flux of atoms diffusing towards the wall must equal the rate of atom mass lost by recombination at the wall. For a first order reaction this results in the equation

$$\rho_w D_w \left( \frac{\partial c}{\partial y} \right)_w = \psi_w (c_w \rho_w)$$

where  $\rho$  = density  
 $D$  = diffusion coefficient  
 $c$  = atom mass fraction  
 $y$  = co-ordinate perpendicular to wall  
 $\psi$  = catalytic reaction rate constant

subscript w denotes conditions at wall.

Goulard proceeded from here to solve the boundary layer equations for the case of frozen flow. He obtained the following expression for the heat transfer rate

$$q = F \left\{ 1 + (\text{Le}^{\frac{2}{3}} \phi - 1) \frac{h_{Rc} e}{h_{se}} \right\}$$

$$\text{where } \phi = \frac{1}{1 + \frac{0.47 \text{Sc}^{-\frac{2}{3}} (2\beta \mu_{se} \rho_{se})^{\frac{1}{2}}}{\rho_w \psi_w}}$$

$$\beta = \frac{2u_{\infty}}{d} \left\{ \frac{\rho_{\infty}}{\rho_{es}} \left( 2 - \frac{\rho_{\infty}}{\rho_{es}} \right) \right\}^{\frac{1}{2}}$$

$$\text{and } \text{Le} = \text{Lewis number} = \frac{\rho D c_p}{k}$$

$h_R$  = heat of recombination

$\text{Sc}$  = Schmidt number =  $\frac{\mu}{\rho D}$

$\mu$  = viscosity

$u_{\infty}$  = velocity ahead of bar shock wave

$d$  = nose diameter

subscripts e denotes conditions outside boundary layer

s denotes stagnation conditions.

F is a function of the flow variable only and will cancel when comparing heat transfer rates to surfaces of different catalytic efficiencies. For the case of  $\phi = 1$  the equation reduces to that obtained by Lees.

Goulard's results were used to calculate the ratio of heat transfer rate for finite catalytic activity to heat transfer rate for infinite catalytic activity. Actual heat transfer rates for several different catalytic activities were also calculated. Shock Mach number and initial channel pressure were used as variables. The equilibrium gas properties at the stagnation point were taken from Ref. 7. The results are given in Figs. 9 and 10.

#### 4. Results

When planning these experiments an order of magnitude analysis was made to decide on suitable pressures to give frozen conditions through the boundary layer. Previous studies of Couette flow by Clarke (Ref. 8) indicated that a stagnation pressure of not more than 0.1 atmospheres should give frozen conditions. This immediately determined the range of initial channel pressures to lie between 0.01 Torr to 0.1 Torr for shock Mach numbers from 15 to 10. Previous experiments indicated that the testing time available would be very short at these low densities due to thick boundary layers. Some measured values, as determined from stagnation point heat transfer records, are given in Fig. 11. This gave reason for concern as it was felt that there would be insufficient time for the flow to become steady. However, heat transfer records show that almost constant heat transfer rate is obtained in most cases. This seems to indicate that the starting processes are very fast and that heat transfer rate at the stagnation point is insensitive to non-equilibrium conditions.

Runs were done initially with only one type of uncoated gauge to check the electrical analogues. By determining the heat transfer rates from Fay and Riddell's curve at the low calibration shock Mach numbers, the heat transfer rates at the higher Mach numbers could be determined. The results have been corrected for variations in initial pressure and are shown in Fig. 12. It can be seen that the results are consistently higher than those predicted by Fay and Riddell. This may be due to a gas adsorption effect which will be discussed later. The important conclusion from these results is that the bare platinum behaves as an efficient catalyst and if the flow is frozen complete recombination must be taking place at the wall.

Experiments were then done with similar models but this time the platinum was coated with silicon monoxide. It was soon realised that because it was impossible to reproduce identical flow conditions in the shock tube, the catalytic effect, which appeared to be small, would be masked by inaccuracies. Consequently the composite model was made so that the two surfaces could be tested under identical conditions. Tests were made using amplifiers with the same sensitivity and rise time, and the heat transfer rates for the two gauges were displayed on the double beam oscilloscope. The calibration runs showed that within the accuracy of measurement the heat transfer rates were the same. This was expected for undissociated flows. However, for flows with appreciable dissociation a difference was observed, the silicon monoxide coated gauge recording a lower heat transfer rate as in Fig. 13. To improve the accuracy of measurement the two signals were fed to a difference amplifier which could be set to a higher sensitivity. At the same time the signal from the uncoated gauge was displayed on the oscilloscope. Fig. 14 shows that the difference for the calibration run is zero, whilst for the dissociated flow there is a positive difference until behind the contact surface when the difference is also zero.

It is apparent, from these results, that the bare platinum and silicon monoxide surfaces have significantly different effects on heat transfer rates in hot dissociated gas flows.



## 5. Comparison of Theoretical and Experimental Results

The following table gives the ratio of heat transfer rates as calculated from Goulard's theory and corresponding experimental values.

$M_s$	$P_1$ (Torr)	$\bar{q}_{exp.}$	$\bar{q}_{theor.}$
8.7	0.052	0.97	0.70
14.6	0.047	0.93	0.42
15.0	0.039	0.84	0.40
16.2	0.024	0.90	0.35
18.1	0.024	0.83	0.34

$$\bar{q} = \frac{\text{Rate of heat transfer to silicon monoxide}}{\text{Rate of heat transfer to platinum}}$$

$$= \frac{q_{\psi_w} = 1}{q_{\psi_w} = 10^3}$$

Although the experimental results show the same trends as theory the reduction in heat transfer rate is not nearly as large as expected. The reason for the smaller difference in the measured values could be one or all of three.

### 5.1. The flow in the boundary layer is not frozen

If partial recombination takes place in the boundary layer then the atom concentration at the wall will be lower than expected. Thus the reduction in heat transfer rate to a non-catalytic wall would be less than for frozen conditions. As a result of this conclusion a more careful estimate using the approximate results in Ref. 8 of the chemical reaction times compared to the atom diffusion times was made. The results are shown in Fig. 13 and for the working pressure range the chemical times are several orders of magnitude greater than the diffusion times. It would appear that under the conditions of the present experiments, the flow is completely frozen at the stagnation point. (This result is also valid for non-equilibrium conditions).

### 5.2. Incorrect value for the catalytic activity of silicon monoxide

There is little doubt that the platinum film, as deposited, is in a highly active catalytic state. It is probable that the catalytic activity is about  $10^4$  cm/sec. as given by Goulard and others (Fig. 10). The catalytic activity of silicon monoxide was taken as one cm/sec. as it was thought that it would behave like a glass and have low catalytic activity. However, even if silicon monoxide has a value characteristic of metallic oxides, i.e. between 10 cm/sec. and  $10^2$  cm/sec. there would be negligible change in the theoretical values as the most marked changes occur between  $10^2$  cm/sec. and  $10^3$  cm/sec. Nevertheless an uncertainty remains as to the correct value of the catalytic activity for silicon monoxide and further experiments need to be made to clarify this point.

### 5.3. The flow outside the boundary layer is not in equilibrium

The argument applied to frozen flow also applies to non-equilibrium conditions where the atom concentration will be lower than the equilibrium value. Cammac and others (Ref. 9) have measured relaxation times for oxygen in shock heated air using ultra violet absorption techniques. These results have been extrapolated to lower pressures and are shown in Fig. 16. It is immediately seen that for the measured flow lengths the flow ahead of the bow shock wave is far removed from equilibrium. Even though the flow will have longer to equilibrate behind the bow shock, where the velocities near the stagnation point are very low, the times involved appear to be too short for the flow to reach equilibrium.

This then appears to be the most probable reason for the discrepancy between theory and experiment, i. e. the assumptions of the theory are not reproduced in practice.

In conclusion there are two additional factors about which little is, at present, known and which may materially affect the flow processes involved in these experiments.

Firstly, it is known that heats of adsorption, i. e. the energy involved when a gas molecule or atom is bound to a solid surface, can be as large as dissociation energies. Little is known of rates of adsorption and whether these are of the same time scale as has been discussed. One of the most recent tests done in the shock tube was to pump the tube down for several hours with the diffusion pump. Fig. 17 shows the heat transfer rates to the two films after prolonged outgassing for three hours. The traces bear little resemblance to the previous traces but after two more runs without prolonged pumping returned to normal. This effect may be due to adsorption.

Secondly, Schlieren photographs show that the bow shock does not reach its final position until about 5 microseconds after the arrival of the primary shock wave. In addition the times required for the boundary layer to become steady are unknown. It is difficult to see at this stage what effect, if any, these processes will have on heat transfer rates near the stagnation point. Nevertheless, it will be necessary to have some knowledge of them if experiments are to be done in such short testing times.

### 6. Acknowledgements

The author wishes to acknowledge useful discussions with J. F. Clarke and the practical help of E. Taylor.

7. References

1. Lees, L.                   Laminar heat transfer over blunt-nosed bodies at hypersonic flight speeds.  
Jet Prop. vol. 26, No. 4, April 1956, pp 259-269.
2. Fay, J.A.,  
Riddell, F.R.               Theory of stagnation point heat transfer in dissociated air.  
J.Aero.Sc. vol. 25, No. 2, Feb. 1958, pp 73-85.
3. Rose, P.H.,  
Stark, W.I.                 Stagnation point heat transfer measurements in dissociated air.  
J.Aero.Sc. vol. 25, No. 2, Feb. 1958, pp 86-97.
4. Scala, S.M.               Hypersonic stagnation point heat transfer to surfaces having finite catalytic efficiency.  
Proc. 3rd U.S. Con.App.Mech. pp 799-806.
5. Goulard, R.               On catalytic recombination rates in hypersonic stagnation heat transfer.  
Jet Prop. vol. 28, No. 11, Nov. 1958, pp 737-745.
6. Meyer, R.F.               A heat-flux-meter for use with thin film surface thermometers.  
N.R.C. of Canada. Aero.Rep.LR-279, April 1960.
7. Feldman, S.               Hypersonic gas dynamic charts for equilibrium air.  
AVCO Research Laboratory, Jan. 1957.
8. Clarke J.F.               Energy transfer through a dissociated diatomic gas in Couette flow.  
ARC Report 19,624, Sept. 1957.
9. Cammac, M. et al.        Chemical relaxation in air, oxygen and nitrogen.  
I.A.S. Preprint No. 802, Jan. 1958.

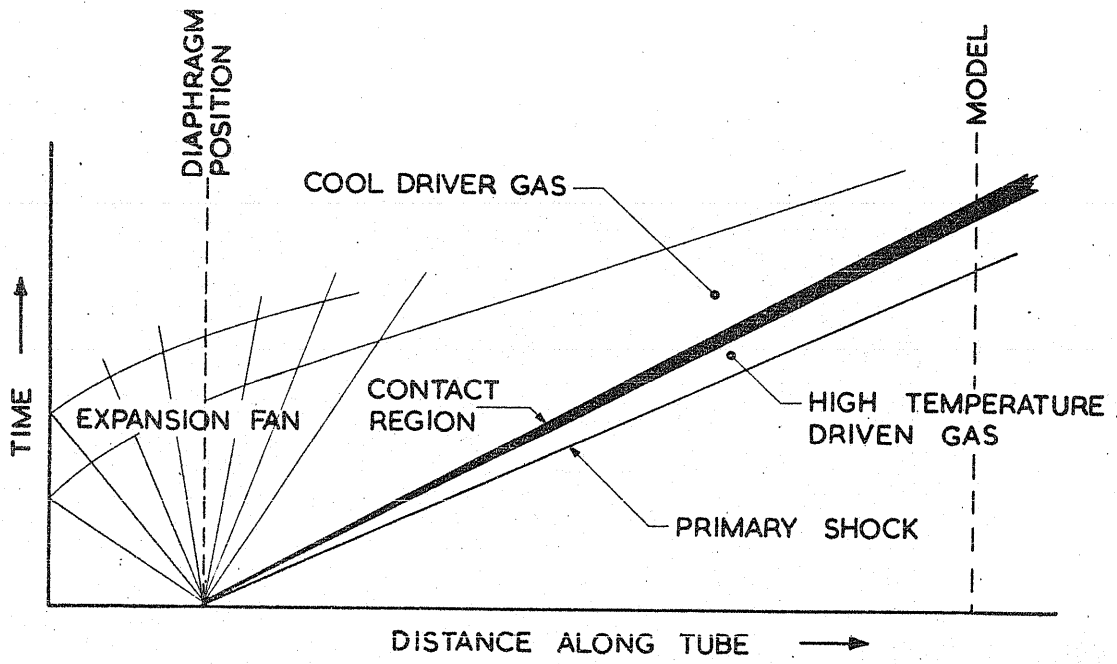


FIG.1. WAVE PROCESSES IN A SHOCK TUBE

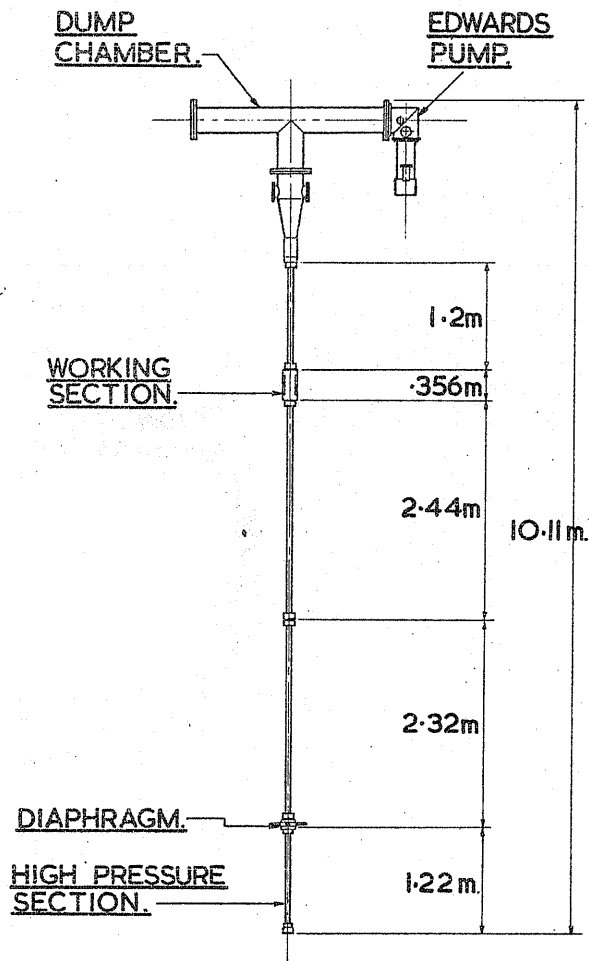


FIG.2. THE COLLEGE OF AERONAUTICS. SHOCK TUBE.

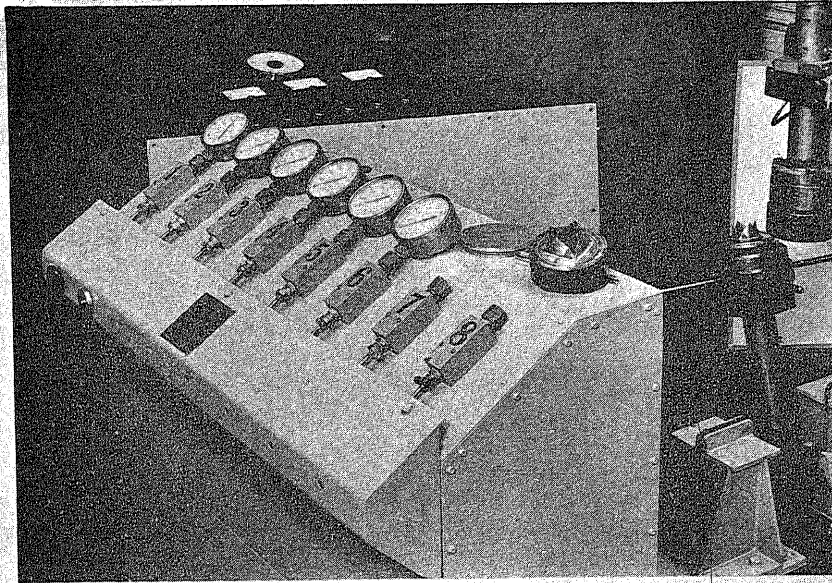


FIG. 3a. CHARGING EQUIPMENT AND HIGH PRESSURE CHAMBER.

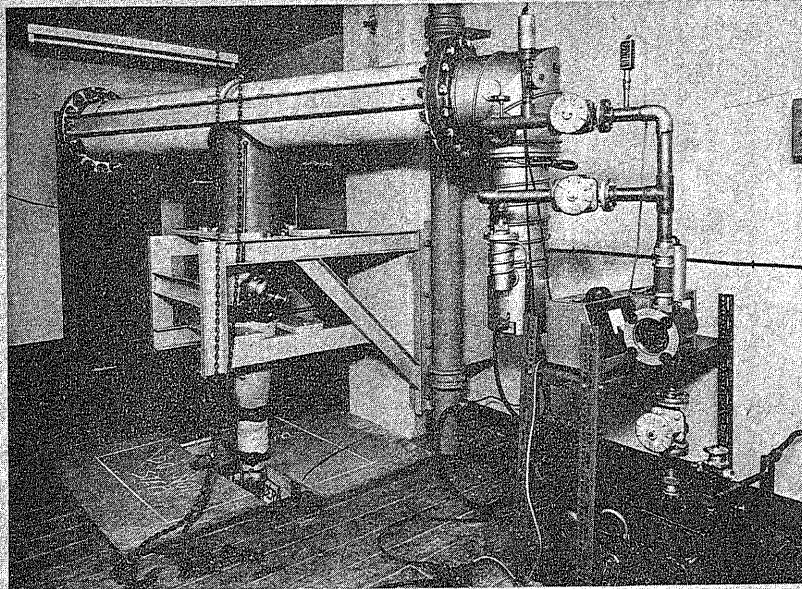


FIG. 3b. DUMP TANK AND PUMPING EQUIPMENT.

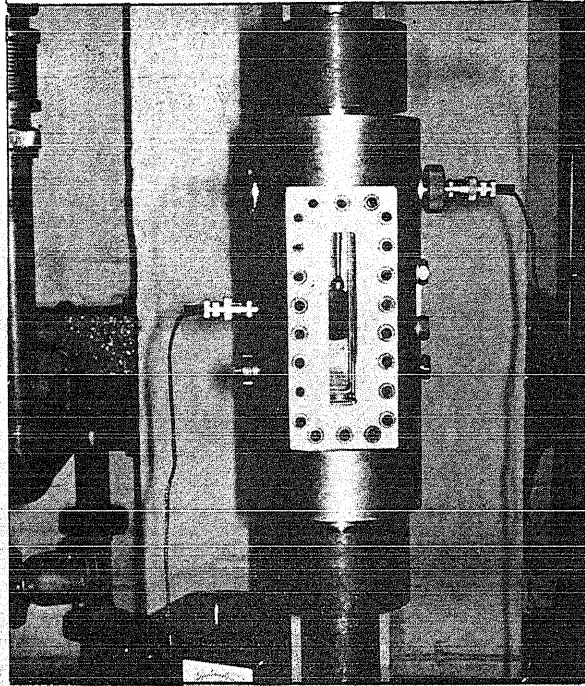


FIG. 4a. MODEL MOUNTED IN WORKING SECTION.

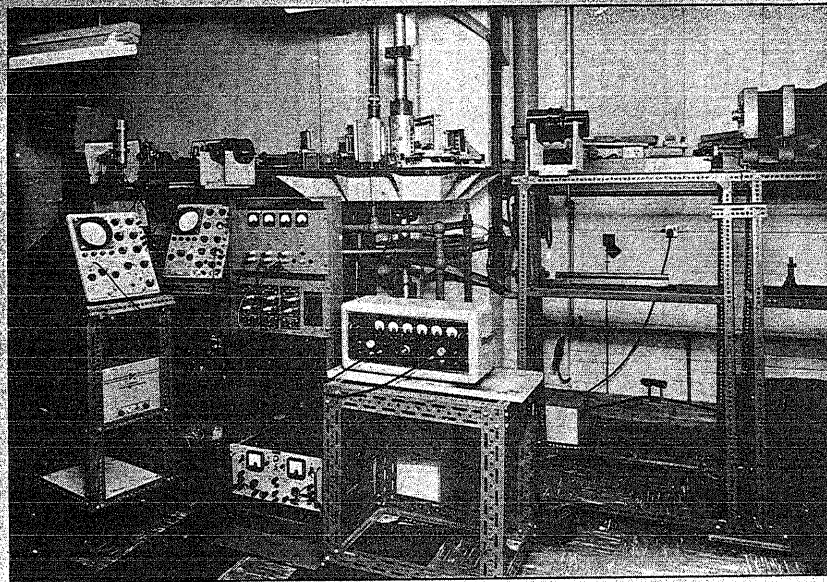
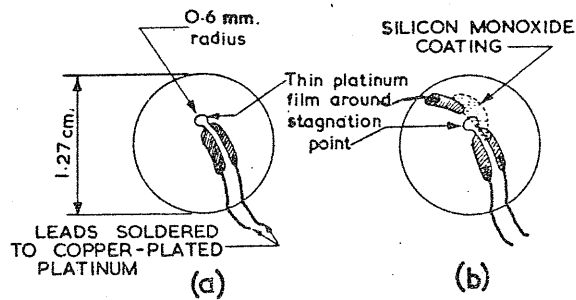


FIG.4b. WORKING SECTION, OPTICAL AND ELECTRONIC EQUIPMENT.



HEAT TRANSFER GAUGES ON PYREX

SPHERE MODELS

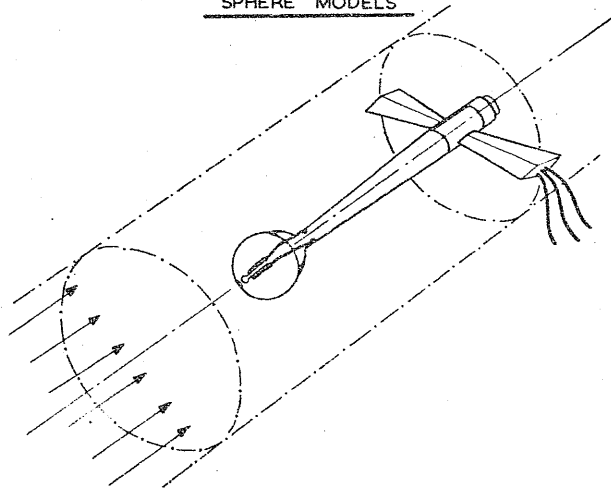
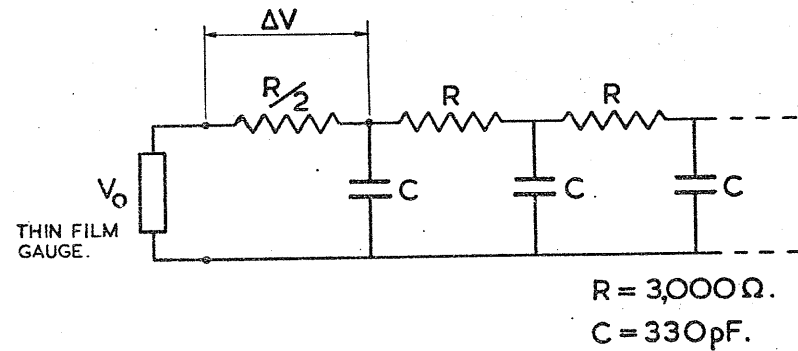


FIG. 5. STING MOUNTING OF MODELS IN SHOCK TUBE



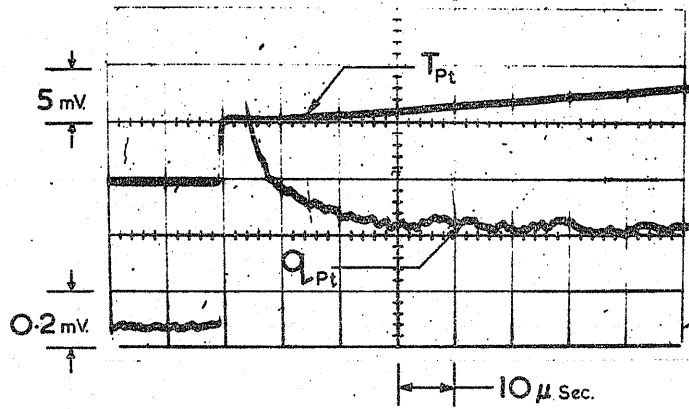
Time constant  $\approx 1 \mu\text{sec}$ .

Running time (24 sections)  $\approx 100 \mu\text{sec}$ .

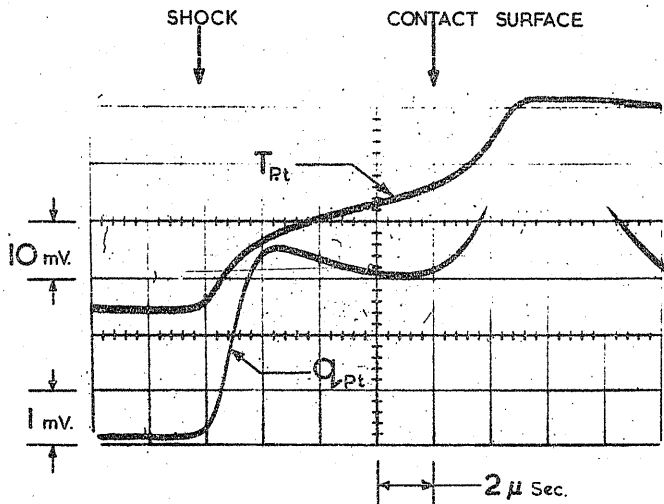
$$q = \frac{\Delta V}{V_0} \left( \frac{\rho C_p k}{\epsilon} \right)^{1/2} \frac{2}{(RC)^{1/2}}$$

where  $q$  = rate of heat transfer.  
 $V_0$  = initial voltage across gauge.  
 $\Delta V$  = output from analogue circuit.  
 $RC$  = time constant of analogue circuit.  
 $\epsilon$  = temperature coefficient of resistance of platinum film.  
 $\rho$  = density of pyrex.  
 $C_p$  = specific heat of pyrex.  
 $k$  = thermal conductivity of pyrex.

FIG. 6. ELECTRICAL ANALOGUE FOR OBTAINING HEAT TRANSFER RATES.



RUN 437 MODEL A  $M_s=2.34$   $p_i=50$  Torr



RUN 438 MODEL A  $M_s=9.45$   $p_i=0.05$  Torr

FIG.7 COMPARISON OF SURFACE TEMPERATURE AND HEAT TRANSFER RATE

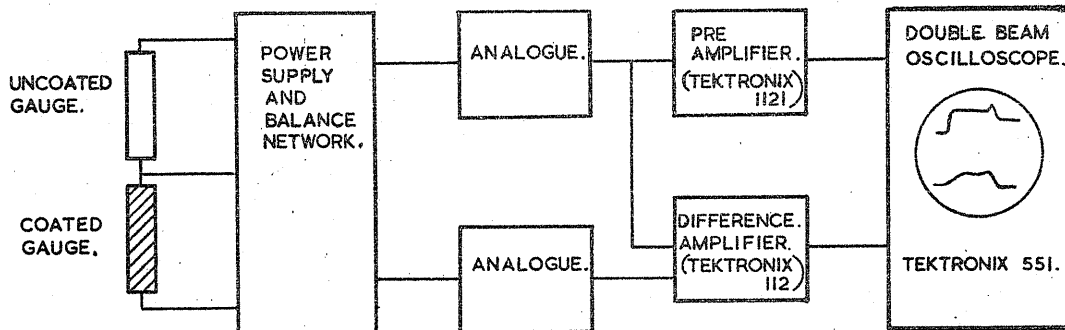


FIG.8. CIRCUIT FOR RECORDING HEAT TRANSFER RATES.



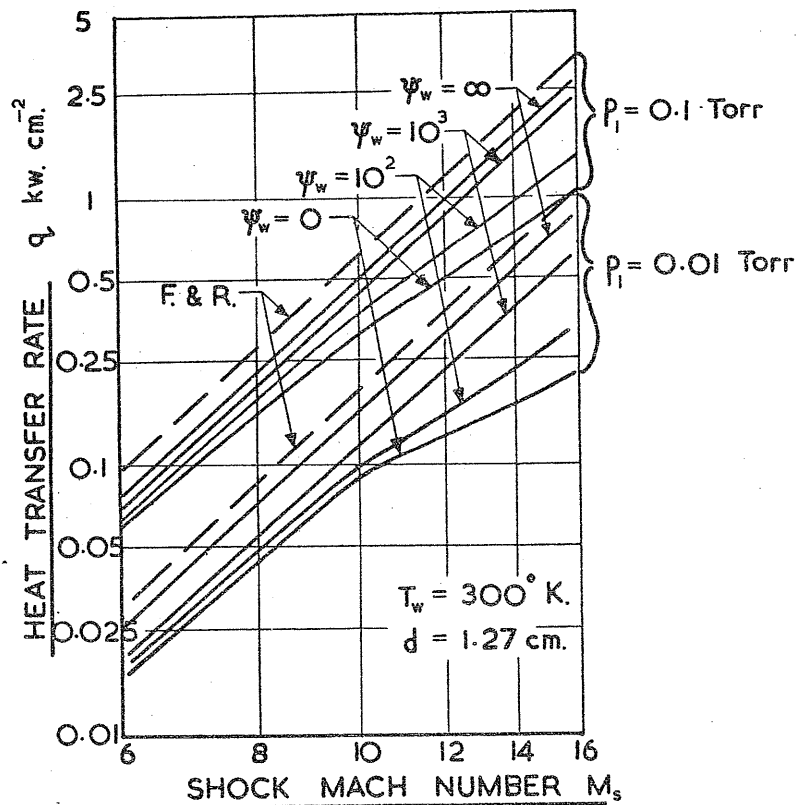


FIG.9. STAGNATION POINT HEAT TRANSFER  
ASSUMING EQUILIBRIUM FLOW OUTSIDE  
BOUNDARY LAYER AND FROZEN FLOW  
THROUGH IT.

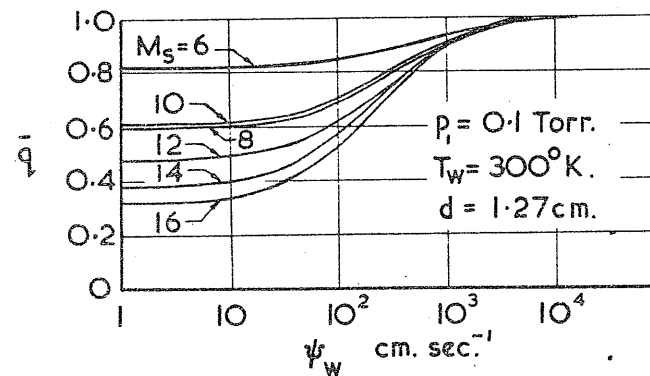
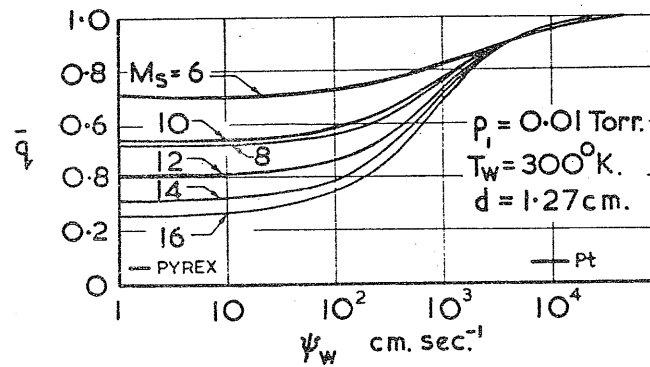


FIG.10. REDUCED HEAT TRANSFER.  $\bar{q} = q/q_{\psi_w = \infty}$

$$\bar{q} = 1 - \frac{Le^{2/3} \frac{hr c_e}{h_{se}}}{1 + (Le^{2/3} - 1) \frac{hr c_e}{h_{se}}} (1 - \phi)$$

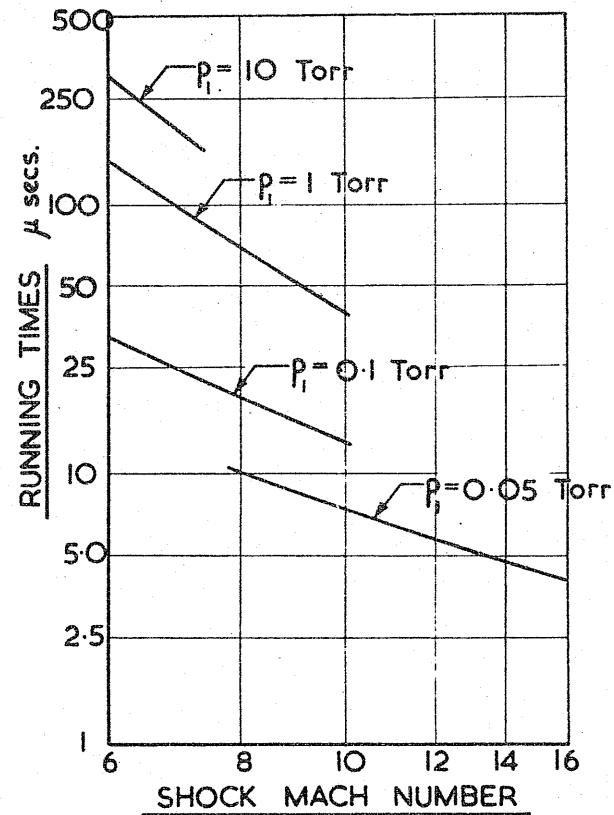


FIG.11. MEASURED RUNNING TIMES IN 5 cm. Dia. SHOCK TUBE AT LOW INITIAL PRESSURE

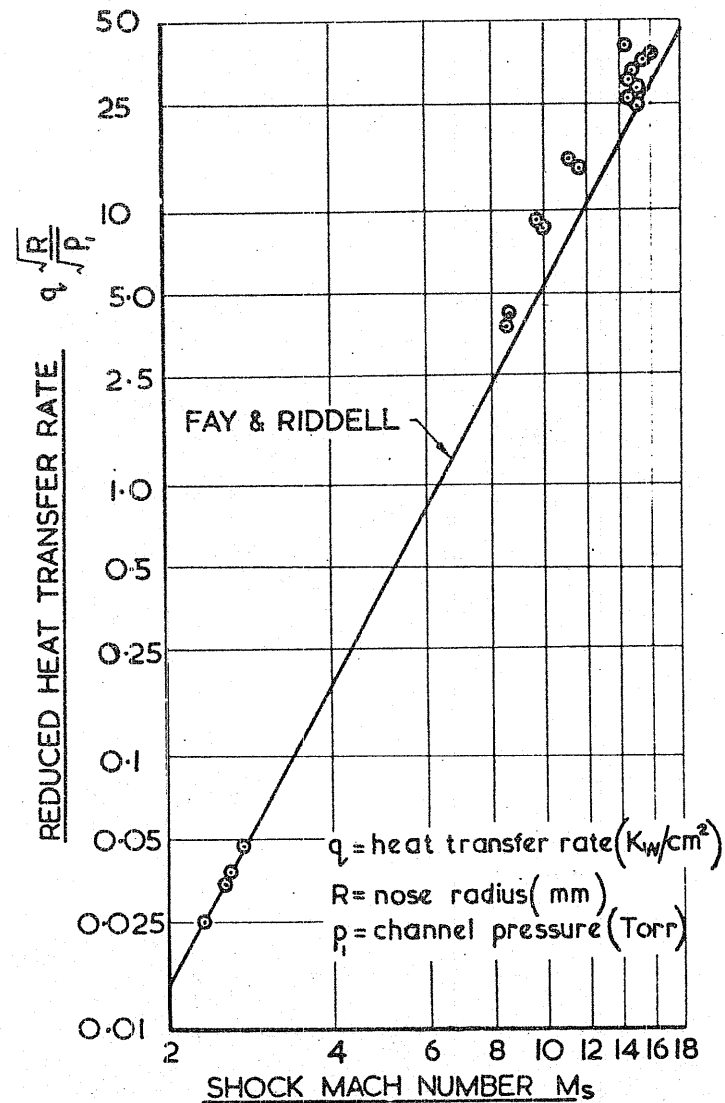
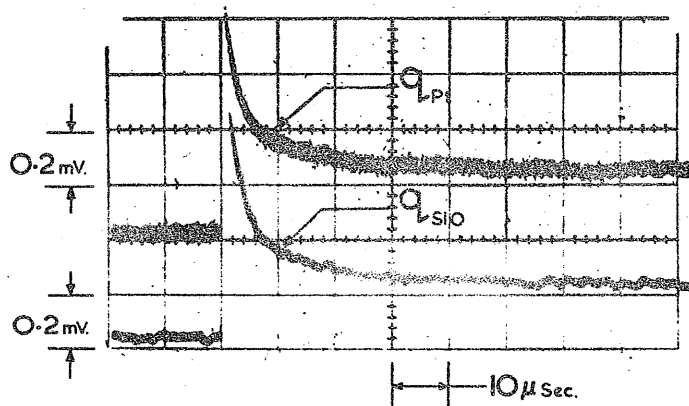
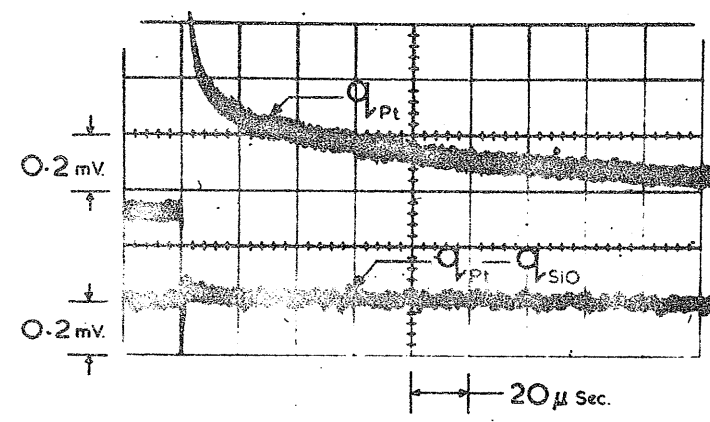


FIG.12. STAGNATION POINT HEAT TRANSFER FOR INITIAL CHANNEL PRESSURES BETWEEN 0.01 Torr AND 0.1 Torr.

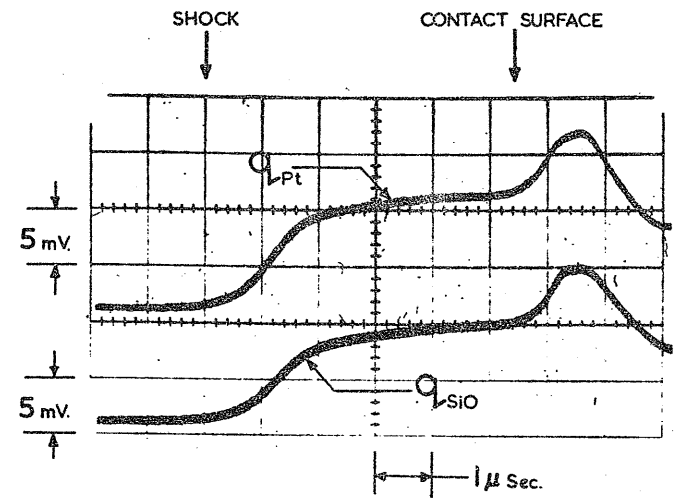




RUN 450 MODEL B  $M_s=233$   $p_i=50$  Torr

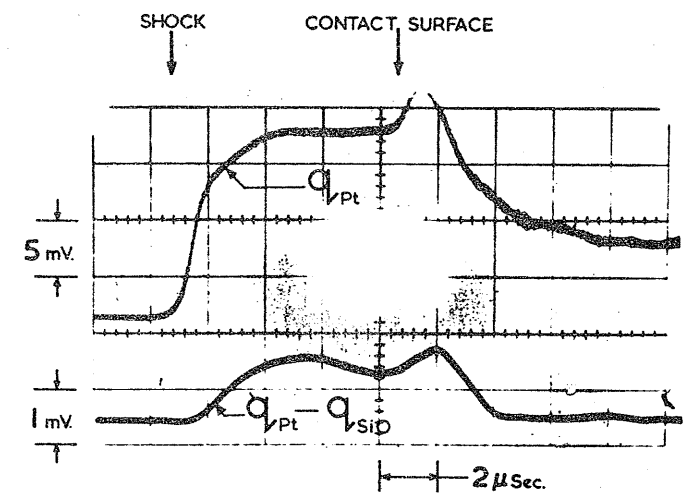


RUN 462 MODEL D  $M_s=2.34$   $p_i=50$  Torr



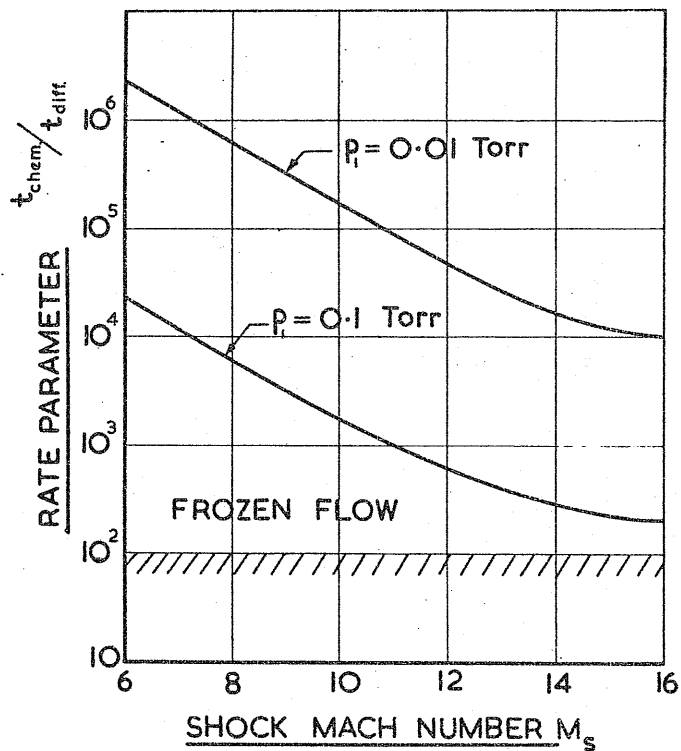
RUN 453 MODEL B  $M_s=16.2$   $p_i=0.024$  Torr

FIG.13. STAGNATION POINT HEAT TRANSFER RATES



RUN 455 MODEL B  $M_s=14.6$   $p_i=0.047$  Torr

FIG.14. STAGNATION POINT HEAT TRANSFER RATES



$$\frac{t_{chem}}{t_{diff}} \sim \frac{10^{-3}}{p^3 \delta^2}$$

Body diameter  $d = 1.27$  cms.

Recombination rate  $k_r = 10^{17} \text{ cc.}^2 \text{ mole}^{-2} \text{ sec.}^{-1}$

Boundary layer thickness  $\delta$

FIG.15. RATE PARAMETER VARIATION WITH MACH NUMBER AND CHANNEL PRESSURE

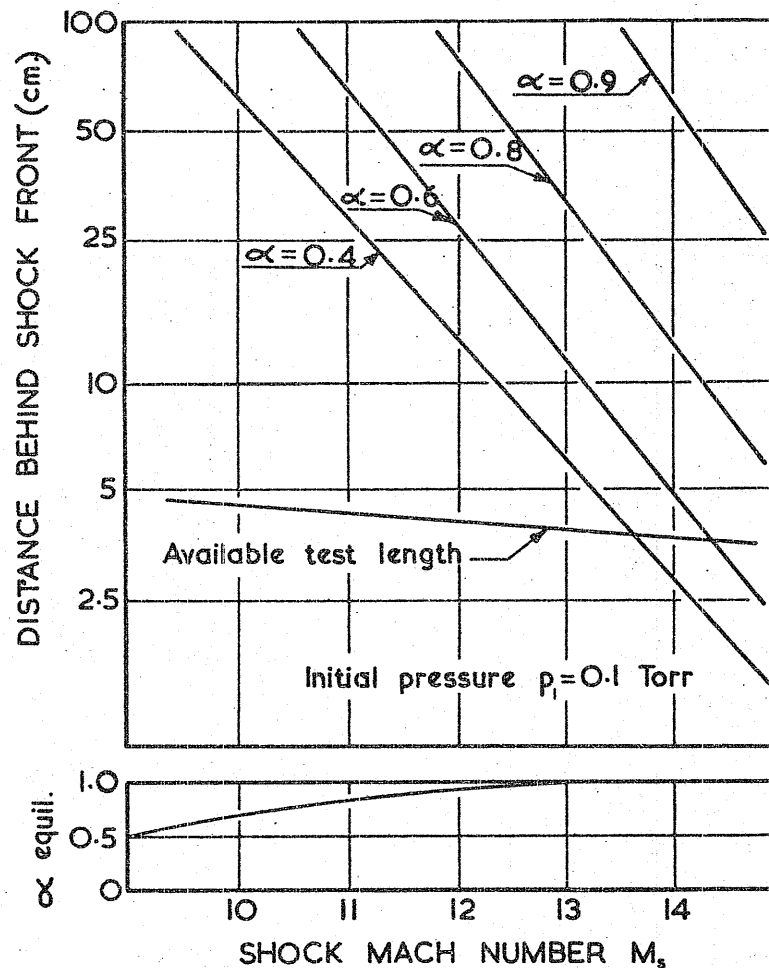
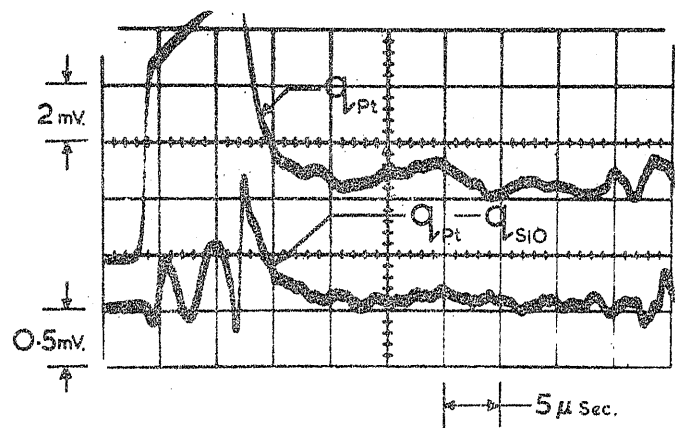


FIG.16. DISTANCE BEHIND SHOCK FRONT FOR OXYGEN TO REACH A GIVEN DEGREE OF DISSOCIATION ( $\alpha$ )



RUN 463    MODEL D     $M_s = 13.1$      $p_i = 0.047$  Torr

FIGURE EFFECT OF PROLONGED OUTGASSING ON  
STAGNATION POINT HEAT TRANSFER RATES